Microarray Analysis of the Failure of Filtering Blebs in a Rat Model of Glaucoma Filtering Surgery

Douglas W. Esson,[1,2] Michael P. Popp,[3] Li Liu,[3] Gregory S. Schultz,[2,4] and Mark B. Sherwood[1,2]

PURPOSE. To generate data concerning changes in levels of protein expression associated with wound healing and bleb failure in a rat model of glaucoma filtration surgery (GFS), and to identify factors that may play a role in this process.

METHODS. Of 36 Sprague-Dawley rats, GFS was performed on 27 by introducing a silicone cannula through a scleral tunnel under a conjunctival flap, resulting in aqueous-filtering blebs that failed over 8 to 13 days. The additional nine rats were used as the nonsurgical control. Nine blebs were harvested at each of days 0, 2, 5, and 12 and pooled, yielding three replicates of three blebs per time point. RNA was extracted, labeled, and hybridized to 230A rat GeneChip arrays (Affymetrix, Santa Clara, CA).

RESULTS. Of the 15,924 probe sets/genes present on the array, 923 genes were indicated to have a significant treatment effect at $P < 0.005$. Eight gene expression clusters were identified that could be broadly classified into three basic patterns. These were an increase on day 2, a decrease on day 2, or an increase on either day 5 or 12. The greatest change occurred between days 0 and 2. The most heavily populated functional categories included growth factors, structural proteins, and matrix metalloproteinases.

CONCLUSIONS. This study represents the first large-scale gene expression analysis after GFS. Expression patterns for known mediators of the bleb scarring process, including transforming growth factor-β, connective tissue growth factor, and matrix metalloproteinases, were confirmed, and a number of mediators not previously associated with this process were identified. (*Invest Ophthalmol Vis Sci.* 2004;45:4450–4462) DOI:10.1167/iovs.04-0375

Worldwide, it is estimated that 65 million people are affected by glaucoma, and it remains a leading cause of blindness.[1–3] The principal risk factor associated with development of vision loss is intraocular pressure (IOP), and, although glaucoma has multiple causes, lowering IOP has been shown to be effective in reducing optic nerve damage.[4–6] When medications fail to control IOP adequately, glaucoma filtering surgery (GFS) may be performed.

The long-term failure of GFS is generally the result of excessive subconjunctival scarring that develops at the site of surgery.[7,8] Scarring can be reduced and the long-term success of GFS enhanced by treatment with antimetabolites, predominately 5-flurouracil (5FU) and mitomycin-C (MMC).[9–11] The action of these compounds, however, is relatively nonspecific, and their use may be associated with an increased incidence of adverse effects including hypotony-maculopathy, bleb leaks, bleb infections, and endophthalmitis.[12–18]

The identification of key molecular mechanisms involved in ocular wound healing, specifically those that occur in the conjunctiva and Tenon's capsule, may facilitate the development of novel treatments to limit the formation of scar tissue. Thus, there is a need for a more comprehensive assessment of changes in gene expression patterns during all the phases of scarring after GFS.

Microarray technology has been extensively used by researchers, to identify the molecular changes underlying the biological processes (including wound healing) that lead to the phenotypic differences observed in cells and organisms.[19–22] The ability of this technology to simultaneously evaluate the expression of tens of thousands of genes, provides an unprecedented ability to study changes in biological systems at a global level, identifying how entire pathways and processes are regulated, coordinated, interconnected, and potentially altered. The utility of microarray technology is limited, however, by the necessity of having an appropriate and well-characterized animal model system.

Although the rat is well established as a model of general,[23–27] corneal,[28–30] and retinal[31] wound healing, the standard animal model for the investigation of wound healing and the scarring process after GFS has been the rabbit, primarily because of the size of the eye.[32–39]

However, unlike the rat, there are no commercially available microarrays for the rabbit at this time. In addition, there are very few expressed sequence tagged (EST) sequences available in public databases from which a rabbit microarray could be developed.[40–42] Although this type of microarray experimental design is theoretically possible using primates,[43–46] such an experiment would be costly and necessitate the killing of a large number of primates. We therefore chose to develop a rat model of GFS with which to investigate changes after GFS at the molecular level.[47]

We have used the new rat model to present the first microarray analysis of changes in gene expression in the conjunctival and Tenon's capsule tissues after GFS, which drains aqueous into a subconjunctival bleb.

MATERIALS AND METHODS

A total of 36 adult, male Sprague-Dawley rats were used for the study. All procedures were conducted in accordance with the ARVO Statement for the Use of Animals in Ophthalmic and Vision Research and were approved by the University of Florida's Institutional Animal Care and Use Committee.

FIGURE 1. Surgical technique. (**A**) Cannula insertion, (**B**) stilet withdrawal, and (**C**) aqueous bead formation.
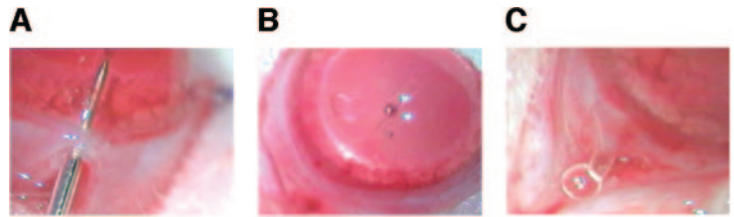
Glaucoma Filtering Surgery

Surgical anesthesia was induced with a mixture of isoflurane (Aerrane; Baxter Healthcare Corp., Deerfield, IL) and oxygen, initially through an induction chamber and subsequently delivered through a standard rodent nonrebreathing anesthetic circuit connected to the animal by face mask. Additional topical anesthesia was provided in the form of 0.5% proparacaine drops (Bausch & Lomb, Tampa, FL).

Eyelids were retracted with two 8-0 traction sutures (Vicryl; Ethicon Inc., Somerville, NJ) and the globe rotated inferiorly by an assistant, using a cellulose sponge (Microsponge; Alcon, Fort Worth, TX) applied to the cornea. A limbus-based conjunctival flap was created 3 to 4 mm behind the limbus by making a conjunctival incision and elevating the underlying Tenon's capsule by blunt dissection. No antimetabolites were applied. A full-thickness scleral tunnel was then created with a 29-gauge needle, which was inserted into the anterior chamber (AC), taking extreme care to avoid the iridal blood vessels. Rats exhibiting any hyphema were not included in the study. Viscoelastic (10 mg/mL, Healon; Pharmacia & Upjohn, Uppsala, Sweden) was injected through the needle to maintain the AC and the needle withdrawn. A beveled 30-gauge over-the-needle microcannula (Fine Science Tools, N. Vancouver, British Columbia, Canada) was then inserted through the scleral tunnel (Fig. 1A). After it was inserted into the AC, the cannula was advanced through the iris tissue into the midpupillary area of the AC, after which the stilet was withdrawn (Fig. 1B). The tight fit of the cannula in the sclera tunnel and iris tissue meant that no anchoring suture was necessary, and none of the eyes in which surgery was performed exhibited subsequent slippage or dislocation of the cannula. The proximal end of the cannula was trimmed flat approximately 1 mm behind the limbus and a bead of fluid visualized to confirm patency (Fig. 1C). The conjunctiva and Tenon's capsule were closed in a single layer, using a nonabsorbable 10-0 suture attached to a blood vessel vascular (BV) needle (Prolene; Ethicon, Somerville, NJ) in a continuous locking pattern. In all cases, a filtering bleb formed immediately after surgery. A single drop of combined anti-inflammatory/antibiotic ointment (Neomycin, Polymyxin, Dexamethasone; Bausch & Lomb) was instilled after surgery. No additional medications were given.

Blebs were observed to be elevated and avascular for the initial 24 to 48 hours after surgery (Fig. 2A), becoming less elevated, fleshy, and more vascularized in appearance by days 4 to 5 (Fig. 2B) and flat by days 8 to 13 (Fig. 2C), which was consistent with the previous experience with this rat model of GFS.[38]

Sample Collection and Preparation of Labeled Copy RNA

Each of nine rats was randomly selected and killed 2, 5, and 12 days after surgery. Bleb tissue from an area measuring approximately 4×4 mm, consisting of conjunctiva and Tenon's capsule was harvested by sharp dissection and immediately placed in individual 1.5-mL microfuge tubes, snap frozen in liquid nitrogen, and stored at $-80°C$. Conjunctival and Tenon's capsule tissue from nine rats that did not undergo surgery was harvested and stored in the same manner and served as the nonsurgical normal tissue control (day 0). The nine independent samples for each day were then randomly placed into three groups of three samples, generating three replicates for each time point (12 pooled samples in total).

Total RNA was extracted from each of the 12 pooled samples and prepared for hybridization according to the GeneChip Expression Analysis Technical Manual (Affymetrix, Santa Clara, CA). Briefly, tissue samples were macerated in lysis buffer and the RNA extracted (RNeasy Mini kit; Qiagen, Inc., Valencia, CA). Eluant was further cleaned and concentrated by using a companion kit (RNeasy MinElute Cleanup; Qiagen, Inc.). The quality of each clean RNA sample was assessed after running 200-ng aliquots through a microchannel RNA analysis chip on a bioanalyzer (RNA 6000 Nano Chip; Agilent Technologies, Palo Alto, CA) and evaluating the relative amounts of 28s and 18s ribosomal peaks.

A 5-μg aliquot of RNA was used as a template for complementary DNA (cDNA) synthesis (Superscript Choice System kit; Invitrogen Life Technologies, Gaithersburg, MD). First-strand synthesis was primed with a T7-(dT)$_{24}$ oligonucleotide primer containing a T7 RNA polymerase promoter sequence on the 5' end (Genset Oligos, La Jolla, CA). Second-strand products were cleaned (GeneChip Sample Cleanup Module; Affymetrix) and used as a template for in vitro transcription (IVT) with biotin-labeled nucleotides (Bioarray High Yield RNA Transcript Labeling Kit; Enzo Diagnostics, Farmingdale, NY). The copy RNA (cRNA) product was cleaned with the cleanup module, and a 20-μg aliquot was heated at 94°C for 35 minutes in fragmentation buffer provided with the cleanup module (Affymetrix).

Array Hybridization

Fifteen micrograms of adjusted cRNA from each sample was hybridized for 16 hours at 45°C to an Affymetrix 230A GeneChip array. After hybridization, each array was stained with a streptavidin-phycoerythrin conjugate (Molecular Probes, Eugene, OR), washed, and visualized with a microarray scanner (Genearray Scanner; Agilent Technologies). Images were inspected visually for hybridization artifacts. In addition, quality assessment metrics were generated for each scanned image and evaluated based on empiric data from previous hybridizations and on the signal intensity of internal standards that were present in the hybridization cocktail. Samples that did not pass quality assessment were eliminated from further analyses.

FIGURE 2. Course of bleb failure. Bleb at (**A**) 24 to 48 hours, (**B**) 4 to 5 days, and (**C**) 8 to 13 days.

TABLE 1. Genes Significantly Affected by Treatment

Acetoacetyl-CoA synthetase
Achaete-scute comp homologue-like 3
    (Drosophila)Actinin, alpha 1
Adaptor protein complex AP-2, alpha 2
    subunit
Adenosine monophosphate deaminase 3
Adenylyl cyclase 6
Adrenergic receptor, beta 2
AIPI
Aldehyde dehydrogenase family 1,
    member A1
Alpha1,2-fucosyltransferase a
Aminopeptidase A
Annexin III (lipocortin III)
Apolipoprotein B editing protein
Apurinic/apyrimidinic endonuclease 1
Aquaporin 5
Asialoglycoprotein receptor 1
ATPase, Ca++ transporting, card/muscle,
    st2
ATPase, Ca++ transporting, ubiquitous
ATPase, vacuolar, 14 kDa
ATP-binding cassette, sub-family G
    (WHITE), member 1
Attractin
Baculoviral IAP repeat-containing 5
    (survivin)
B-cell receptor-associated protein 37
Bcl2-associated X protein
Biglycan
Bone morphogenetic protein 6
Bone morphogenetic protein 6
Brain acyl-CoA hydrolase
Branched chain aminotransferase 2,
    mitochondrial
BRCA1-associated RING domain protein 1
C1-tetrahydrofolate synthase
Calbindin 3
Calcium channel, voltage-dependent, alpha
    1C subunit
Calmodulin 1 (phosphorylase kinase,
    delta)
Calmodulin 2 (phosphorylase kinase,
    delta)
Calpain 8
Camello-like 5
Carbonic anhydrase 2
Carbonic anhydrase 2
Carbonyl reductase 1
CASP8 and FADD-like apoptosis regulator
Catalase
Cathepsin S
Caveolin
CCA2 protein
CD36 antigen (collagen 1 recpt,
    thrombospondin recpt)-like 2
CD38 antigen
CD44 antigen
CD86 antigen
CDK105 protein
Cell cycle protein p55CDC
Cell cycle protein p55CDC
Cell cycle protein p55CDC
Cell division cycle 2 homologue A (S.
    pombe)
Cell division cycle 25B
Cell division cycle 37 homologue (S.
    cerevisiae)
Cellular nucleic acid-binding protein
Cellular retinoic acid-binding protein 2
Checkpoint kinase 1 homologue (S.
    pombe)

Chloride channel K1-like
Cholecystokinin
Chondroitin sulfate proteoglycan 6
Clathrin, light polypeptide (Lcb)
Claudin 1
Cofilin 1
Cofilin 1
Collagen, type I, alpha 1
Collagen, type I, alpha 1
Collagen, type III, alpha 1
Collagen, type XVIII, alpha 1
Comp/component 1(q subcomp)-binding
    protein
Connective tissue growth factor
Cyclin B1
Cyclin B1
Cyclophilin B
Cysteine rich protein 2
Cytochrome c, somatic
Cytochrome c, somatic
Cytochrome P450 4F4
Cytochrome P450, 2b19
Cytochrome P450, subfamily 2F,
    polypeptide 1
DEAD/H (Asp-Glu-Ala-Asp/His) box
    polypeptide 20
Deoxyuridinetriphosphatase (dUTPase)
Dihydrofolate reductase
DNA ligase 1
DOC2/DAB2-interactive protein
Dodecenoyl-coenzyme A delta isomerase
Drebrin 1
Dystrophin-related protein 2 A-form splice
    variant
Early growth response 2
Ectonucleoside triphosphate
    diphosphohydrolase 6
ElaC homologue 2 (E. coli)
Embigin
Enolase 1, alpha
Eukaryotic translation initiation factor2B,
    subunit3 (gamma)
Exportin 1 (CRM1, yeast, homologue)
Fasting-inducible integral membrane protein
    TM6P1
Fatty acid binding protein 5, epidermal
Fibronectin 1
FK506-binding protein 1a
FK506-binding protein 1a
Follicle-stimulating hormone primary response
    gene 1
For proteasomal ATPase (SUG1)
Fucosidase, alpha-L-1, tissue
Fumarate hydratase 1
FXYD domain-containing ion transport
    regulator 7
G protein-coupled hepta-helical receptor
    Ig-Hepta
G protein-coupled receptor 37 (endothelin
    receptor type B-like)
G protein-coupled receptor 85
Gap junction membrane channel protein
    alpha 4
GCIP-interacting protein p29
Germinal histone H4 gene
Glutamate cysteine ligase, modifier subunit
Glutathione S-transferase, alpha 1
Glutathione-S-transferase, alpha 2
Glycine cleavage system protein H
    (aminomethyl carrier)
Growth arrest and DNA-damage-inducible 45
    alpha

GrpE-like 1, mitochondrial
H2A histone family, member Z
Heat shock 10 kDa protein 1
Heat shock protein 60 (liver)
Heat shock protein 86
Heme oxygenase
Heme oxygenase 2
Hepatoma-derived growth factor
Heterog nuc ribonucleoprotein A1
heterog nuc ribonucleoprotein M
Heterog nuc ribonucleoproteins
    methyltransferase-like 2
High-mobility group AT-hook 1
High-mobility group box 2
Histone 2a
HLA-B-associated transcript 1A
HRAS-like suppressor
Hyaluronan mediated motility receptor
    (RHAMM)
Hypoxia-inducible factor 1, alpha subunit
Inositol 1,4,5-triphosphate receptor 1
Inositol polyphosphate phosphatase-like 1
Inositol polyphosphate-4-phosphatase, type 1
Insulin-like growth factor binding protein 3
Insulin-like growth factor binding protein 3
IP63 protein
Islet cell autoantigen 1, 69 kDa
Isopentenyl-diphosphate delta isomerase
Karyopherin (importin) alpha 2
Killer cell lectin-like receptor subfamily C,
    member 1
Kinase substrate HASPP28
Kinesin heavy chain member 2
Kruppel-like factor 15
Kruppel-like factor 9
Lactate dehydrogenase 3, C chain
Lactate dehydrogenase A
Lactate dehydrogenase B
Lamin A
Lamin B receptor
Lamin B1Laminin 5 alpha 3
Latexin
Lectin, galactose binding, soluble 1
Lumican
Malate dehydrogenase, mitochondrial
Mannosidase 2, alpha 1
Matrix Gla protein
MMP 3
MMP 9 (gelatinase B, 92-kDa type IV
    collagenase)
MMP 9 (gelatinase B, 92-kDa type IV
    collagenase)
Menage a trois 1
Methylmalonate semialdehyde dehydrogenase
    gene
Mg1 protein
Microtubule-associated protein, RP/EB family,
    member 1
Microtubule-associated protein, RP/EB family,
    member 1
Mini chromosome maintenance deficient 6
    (S. cerevisiae)
Mismatch repair protein
Mitochondrial intermediate peptidase
Mitogen-activated protein kinase 1
Mitogen-activated protein kinase kinase 1
Myosin 5a
NADH/NADPH mitogenic oxidase subunit p65-mox
Neural precursor cell-expressed (devel) down-reg'd
    gene 4A
Neural precursor cell-expressed (devel) down-reg'd
    gene 8

(continues)

TABLE 1. (*continued*). Genes Significantly Affected by Treatment

Neuregulin1
Neurofascin
Neurogranin
Nogo-A
Nogo-A
NonO/p54nrb homologue
NonO/p54nrb homologue
Nopp140-associated protein
Nuclear distribution gene C homologue (Aspergillus)
Nuclear distribution gene E homologue (Aspergillus)
Nuclear pore glycoprotein 62
Nuclear pore membrane glycoprotein 210
Nuclear receptor subfamily 3, group C, member 2
Nuclear RNA helicase, DECD variant of DEAD box family
Nuclear transcription factor - Y beta
Nucleolar phosphoprotein p130
Nucleolar phosphoprotein p130
Nucleolin
Nucleophosmin 1
Nucleophosmin 1
Nucleophosmin 1
Nucleoporin 153 kDa
Nucleoporin 155 kDa
Nucleoside diphosphate kinase
Nucleosome assembly protein 1-like 1
Nucleosome assembly protein 1-like 1
Ornithine decarboxylase antizyme inhibitor
Orphan seven transmembrane receptor
Outer mitochondrial membrane receptor rTOM20
p32-subunit of replication protein A
Palmitoyl-protein thioesterase
Peptidyl arginine deiminase, type 4
Phosphatase and tensin homologue
Phosphoglycerate kinase 1
Phosphoglycerate mutase 1
Phospholipase A2, group 10
Phospholipase C, gamma 2
Phosphoribosyl pyrophosphate amidotransferase
Phosphoribosylaminoimidazole carboxylase
Pituitary tumor-transforming 1
Plasma glutamate carboxypeptidase
Pleiomorphic adenoma gene-like 1
Pleiotrophin (heparin-binding factor, Hbnf, in the mouse)
Polo-like kinase homologue (Drosophila)
Polymeric immunoglobulin receptor
Potassium voltage-gated channel, KQT-like subfamily, member 1
Potassium voltage-gated channel, subfamily H, member 3
Procollagen, type I, alpha 2
Procollagen, type I, alpha 2
Profilin II
Profilin II
Prohibitin
Prolactin
Proliferating cell nuclear antigen
Prostaglandin-endoperoxide synthase 1
Protease (prosome, macropain) 26S subunit, ATPase 1
Proteasome (prosome, macropain) subunit, alpha type 3

Proteasome (prosome, macropain) subunit, alpha type 5
Proteasome (prosome, macropain) subunit, beta type, 7
Protein phosphatase 2, regulatory subunit B,B isoform
Protein-L-isoaspartate (D-aspartate) O-methyltransferase
Putative cell surface antigen
Putative c-Myc-responsive
Putative G protein-coupled receptor snGPCR32
Pyridoxine 5-phosphate oxidase
Pyruvate kinase, muscle
Quinoid dihydropteridine reductase
R. norvegicus mRNA for cytokeratin type 1 (3′ end)
R. norvegicus mRNA for novel circadian gene, clone SCN8
Rabin 3
RAN, member RAS oncogene family
RASD family, member 2
Ras-like protein
Rat PMSG-induced ovarian mRNA, 3′sequence, N7
R norveg a/sense RNA overlap/ MCH protein mRNA
R norvegicus cytoplasmic prot bystin mRNA
R norveg hseat shock prot 90 b mRNA
R norveg kinesin-like protein KIF15 mRNA
R norveg kinesin-related protein KRP1 (KRP1) mRNA
R norveg mRNA for hnRNP protein, partial
R norveg mRNA for MHC class I-related protein, Mrl
R norveg phosphoserine aminotransferase mRNA
R norveg vitA-deficient testicular prot 21-like mRNA
R norveg vitA-deficient testicular prot 7-like mRNA
Reelin
Renin 1
Replication factor C (activator 1) 2 (40 kDa)
Reticulocalbin 2
Retinoblastoma binding protein 7
Retinol dehydrogenase 10 (all-trans)
Rgc32 protein
Ribosomal protein L13
Ribosomal protein L14
RING finger protein LIRF
RNA binding protein p45AUF1
RS21-C6 protein
ruvB-like protein 1
S100 calcium-binding protein A4
S6 kinase
S-adenosylhomocysteine hydrolase
Scaffolding protein SLIPR
Scaffolding protein SLIPR
Secreted acidic cystein-rich glycoprotein (osteonectin)
Selective LIM binding factor
Selenium-binding protein 2
Selenoprotein W muscle 1
Seminal vesicle protein, secretion 2
Sepiapterin reductase
Serine threonine kinase 39 (STE20/SPS1 homologue yeast)
Serine/threonine kinase 12
Serine/threonine kinase 6

Sialyltransferase 1 (b-galactoside alpha-2,6-sialyltransferase)
Small inducible cytokine A2
Small nuclear ribonucleoprotein polypeptides B and B1
Sm muscle-specific 17 b-hydroxysteroid dehydrogenase type 3
Sodium channel, nonvoltage-gated 1, gamma (epithelial)
Solute carrier family 11 member 2
Solute carrier family 16, member 1
Solute carrier family 2, member 1
Solute carrier family 21 (fatty acid transporter), member 7
Solute carrier family 21, member 13
Sphingomyelin phosphodiesterase 3, neutral
Staufen, RNA-binding protein, homologue 2 (Drosophila)
Stress-induced-phosphoprotein 1 (Hsp70/Hsp90-organizing)
Structure-specific recognition protein 1
Sulfite oxidase
Synaptojanin 2-binding protein
Synaptojanin 2-binding protein
Syndecan 2
System N1 Na+- and H+-coupled glutamine transporter
System N1 Na+- and H+-coupled glutamine transporter
Tachykinin 1 receptor
T-complex 1
Thymidine kinase 1
Thymidylate synthase
Thymoma viral proto-oncogene 3
Thymopoietin
Timeless (Drosophila) homologue
Tissue inhibitor of metalloproteinase 2
Topoisomerase (DNA) 2 alpha
Topoisomerase (DNA) 2 alpha
Transforming growth factor beta-stimulated clone 22
Translation elongation factor 1-delta subunit
Translation initiation factor eIF-2B alpha-subunit
Translocase (inner mito membrane 8) (yeast) homologue X
Transmembrane domain protein regulated in adipocytes
Tricarboxylate carrier-like protein
Triosephosphate isomerase 1
Tubulin, beta 5
Tubulin, beta 5
Tubulin, gamma 1
Tumor-associated protein 1
Tyrosine 3-m/oxgenase/tryptophan 5-monooxgenase act protein
Ubiquitin-conjugating enzyme
Ubiquitin-conjugating enzyme E21
UDP-glucose dehydrogeanse
Uridine-cytidine kinase 2
Vacuolar protein-sorting protein 4a
Vesicle-associated membrane protein 5
Vimentin
Visinin-like 1
Visinin-like 1
V-myc avian myelocytomatosis viral oncogene homologue
Xanthine dehydrogenase
Zuotin-related factor 2

P < 0.005. Gene names are those assigned to Affymetrix probe set numbers and were obtained from the Affymetrix NetAffx database.
* More than one annotation for the same gene represents multiple probe sets.

TABLE 2. Annotated Genes with a Significant Treatment Effect

Gene Name	Day 0	Day 2	Day 5	Day 12
Achaete-scute comp homologue-like3 (Drosophila)	304.5	43.0	77.4	84.1
Adenosine monophosphate deaminase 3	47.4	253.2	131.1	79.9
Aminopeptidase A	47.2	−3.2	26.4	27.3
Asialoglycoprotein receptor 1	31.3	0.3	6.2	4.4
Biglycan	68.8	158.9	601.7	500.1
BRCAI-associated RING domain protein 1	−1.5	16.8	2.3	−2.1
Carbonic anhydrase 2	14.1	168.4	56.1	10.2
Carbonic anhydrase 2	32.8	192.7	86.5	41.4
Cellular retinoic acid-binding protein 2	20.2	584.2	373.0	188.3
Collagen, type I, alpha 1	41.4	133.0	841.1	688.1
Collagen, type I, alpha 1	79.8	208.7	1251.5	1032.3
Collagen, type III, alpha 1	143.7	478.9	1486.7	1406.3
Collagen, type XVIII, alpha 1	20.6	281.7	187.2	83.9
Connective tissue growth factor	75.4	205.6	391.4	205.7
Cysteine rich protein 2	4.1	47.4	188.5	72.7
Cytochrome P450, 2b19	409.9	65.9	120.9	84.2
Cytochrome P450, subfamily 2, polypeptide 1	444.8	47.6	275.1	180.7
Dystrophin-related protein 2 A (splice variant)	5.3	31.9	275.1	3.5
Fatty acid-binding protein 5, epidermal	86.7	1032.4	794.7	431.6
Fibronectin 1	45.9	232.3	789.5	718.4
Forkhead box MI	2.8	30.0	0.2	−5.2
G/prot-coupled receptor 37 endothelin receptor type B	34.7	5.0	7.8	7.7
Germinal histone H4 gene	73.2	7.0	40.1	35.2
Insulin-like growth factor-binding protein 3	5.5	59.7	45.1	17.7
Insulin-like growth factor binding protein 3	8.0	104.3	64.4	29.4
K voltage-gated channel Shaw-related s/fam	12.4	−16.7	−4.0	−9.3
Lactate dehydrogenase 3, C chain	3.4	27.0	11.8	3.5
Laminin 5 alpha 3	32.5	199.9	95.8	47.2
Lectin, galactose binding, soluble 1	63.6	141.5	562.7	370.8
Lumican	110.3	219.0	683.8	562.7
Lymphocyte antigen 68	1.4	5.1	12.6	4.5
Matrix Gla protein	122.7	900.5	1138.1	737.3
Matrix metalloproteinase 2 (type IV collagenase)	44.7	93.5	332.7	329.4
Matrix metalloproteinase 3	56.3	217.0	291.9	140.1
MMP 9 (gelatinase B, type IV collagenase)	4.5	42.3	52.1	11.7
MMP 9 (gelatinase B, type IV collagenase)	0.6	23.7	26.8	4.8
Myosin 5a	6.6	36.3	29.5	17.5
NADH/NADPH mitogenic oxidase s/unit p65	42.9	5.5	10.6	41.2
Plasma glutamate carboxypeptidase	172.7	5.7	89.6	126.0
Polo-like kinase homologue (Drosophila)	20.7	163.5	44.6	16.7
Polymeric immunoglobulin receptor	935.8	106.8	288.1	522.3
Procollagen, type I, alpha 2	98.5	206.6	1244.5	973.6
Putative c-Myc-responsive	4.5	55.9	4.2	−8.5
Pyridoxine 5-phosphate oxidase	33.7	−4.3	15.6	19.6
Renin I	5.5	43.1	27.4	32.0
Rgc32 protein	4.4	8.3	28.2	19.3
S100 calcium-binding protein A4	58.9	403.8	523.3	461.2
Secreted cystein-rich glycoprotein (osteonectin)	70.0	186.0	695.2	539.4
Selenium-binding protein 2	253.2	26.9	93.0	84.1
Serine/threonine kinase 6	13.3	69.6	26.2	17.5
Small inducible cytokine A2	−8.3	98.5	65.7	95.8
Solute carrier family 16, member 1	18.9	136.0	72.8	41.6
Transmembrane domain protein	33.0	5.2	25.8	19.9
Tumor-associated protein 1	11.9	61.5	39.3	29.6
Vimentin	166.5	602.9	926.6	627.8

P < 0.005. Listed are genes that exhibited a fivefold or greater change in mean signal value (*n* = 3) relative to day 0 (nonsurgical controls).

Generation of Expression Values

Microarray Suite, version 5 (Affymetrix), was used to generate *.cel files, and a computer program (Probe Profiler, ver. 1.3.11; Corimbia Inc., Berkeley, CA) developed specifically for the GeneChip system (Affymetrix) was used to convert intensity data into quantitative estimates of gene expression for each probe set. The software identifies informative probe pairs, and down-weights the signal contribution of probe pairs that are subject to differential cross-hybridization effects or that consistently produce no signal. The software also detects and corrects for saturation artifacts, outliers, and chip defects. A probability statistic was generated for each probe set. The probability is associated with the null hypothesis that the expression level of the probe set is equal to zero (background). Genes not significantly expressed above background in any of the samples (*P* > 0.05) were considered absent. Absent genes were removed from the data set and not included in further analyses.

Data Analysis

Tests of Significance. Gene expression levels were subjected to a one-way analysis of variance (ANOVA) for four treatments (0, 2, 5, and 12 days) and three replications using AnalyzeIt Tools (http://genomics3.biotech.ufl.edu/AnalyzeIt/AnalyzeIt.html), a custom soft-

A

B
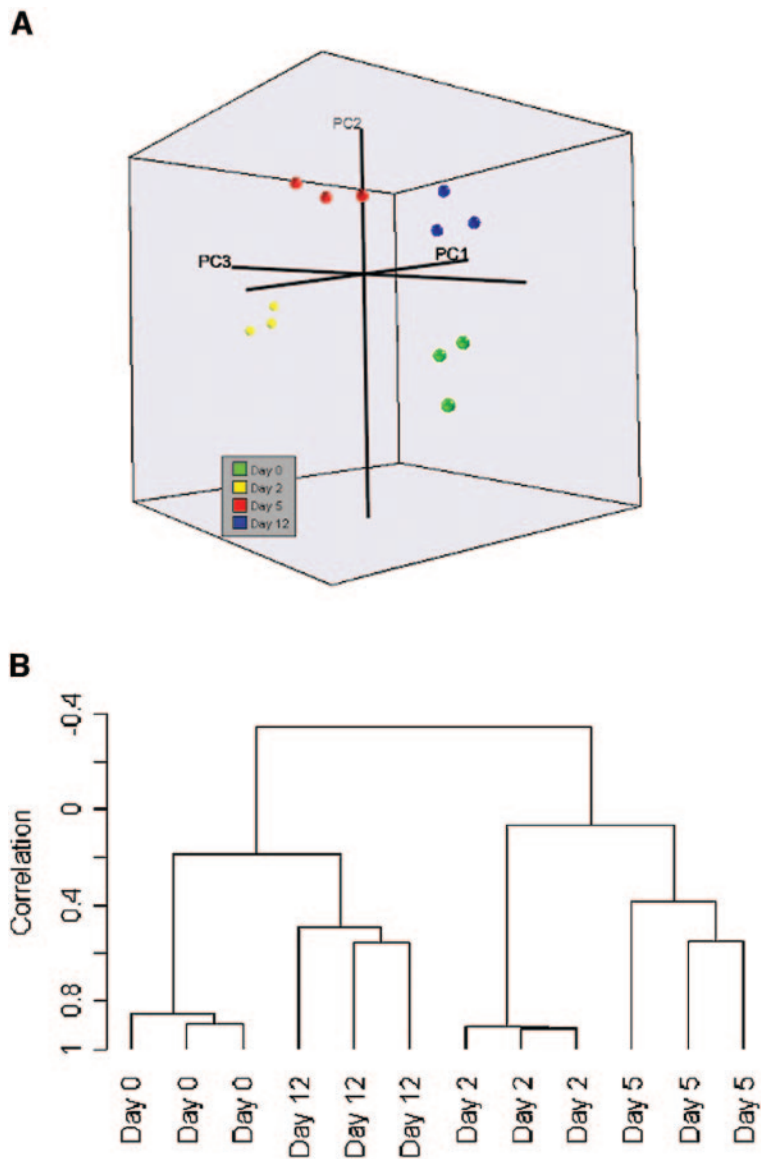
FIGURE 3. (**A**) PCA of the normalized signal values from genes with a significant ($P < 0.005$) treatment effect (time since surgery). (**B**) Agglomerative hierarchical clustering of samples. Only the normalized signal values of genes with a significant ($P < 0.005$) treatment effect (time since surgery) were included. The Pearson correlation coefficient was used to cluster samples with similar expression patterns. Average linkage was used to measure distance between points and clusters. *Lines* in the dendrogram represent a measure of difference. *Longer lines* represent greater dissimilarity between samples.

ware program developed by the Interdisciplinary Center for Biotechnology Research (ICBR; University of Florida) for the analysis of microarray data. In this software, the statistical package, R, serves as the back end for ANOVA. Gene expression levels were also subjected to a multivariate permutation test using BRB Array Tools (provided in the public domain by the National Center for Biotechnology Information, Bethesda, MD at http://linus.nci.nih.gov/BRB-ArrayTools.html). Genes were considered to have a significant treatment effect if the probability for both the ANOVA and the permutation analysis was <0.005.

The expression values of those genes that were considered to have a significant treatment effect were normalized by performing a *Z*-transformation, thereby generating a distribution with a mean of 0 and SD of 1 for each gene. *K*-means clustering and principal component analysis (PCA) were performed on normalized values (GeneLinker Gold 3.1; Predictive Patterns, Kingston, Ontario, Canada), and hierarchical clustering was performed with BRB Array tools.

Gene Annotations. Lists of probe sets (genes) associated with specific aspects of wound healing were generated by conducting queries of the NetAffx database (Affymetrix). Associations are based on the Gene Ontology Consortium's annotations, which has defined terms to describe gene product attributes. AnalyzeIt Tools was used to merge annotations with expression data. In this way we were able to evaluate

wound healing at a more global level by identifying pathways and processes that may be interconnected.

RESULTS

Gene Expression Is Affected by Treatment

Of the 15,924 probe sets (genes) present on the Affymetrix rat 230A array, 13,725 were detected above background on at least one of the arrays. Of those genes, the expression of 923 was significantly affected ($P < 0.005$) by the treatment (postoperative days). The false discovery rate for this analysis was 7.4%. The 923 probe sets identified as being significantly affected by treatment were divided into 344 that had a functional annotation (Table 1), 142 that had a strong similarity to an annotated gene, 212 that had either a moderate or weak similarity to an annotated gene, and 216 that had no annotation.

Ninety-two genes that were significantly affected by treatment had a greater than fivefold change in expression level, relative to that of the nonsurgical control, at the 2-, 5-, or 12-day sampling period (Table 2). Forty-one percent of these genes[38] had no annotation. However, as expected, many of are com-
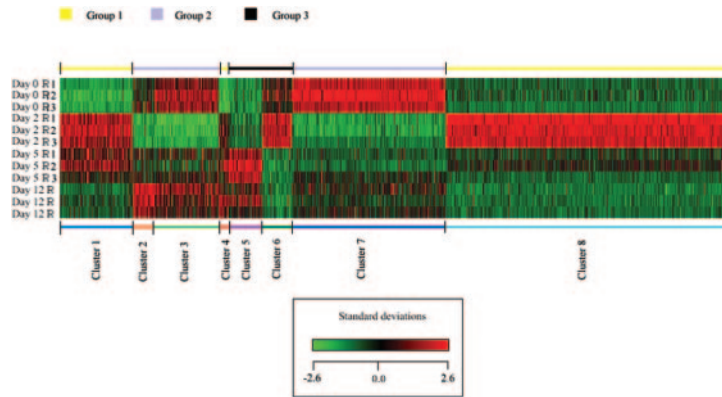
FIGURE 4. *K*-means cluster of normalized signal values for genes with a significant (*P* < 0.005) treatment effect (time since surgery). The Pearson correlation coefficient was used as a distance measurement between points and average linkage used as a measurement between clusters. Each row represents a sample and each column a gene. The scale represents standard deviations from the mean after a *Z*-transformation of signal values of a gene across all samples. *Red* represents a higher level of gene expression and *green* a lower level, relative to the mean across all samples for each gene. The *line* and *bash marks* below mark the boundary between individual clusters and above represent more general expression patterns.

monly associated with wound healing, such as structural proteins, growth factors, and enzymes.

Clustering Gene Expression Patterns

PCA was performed to identify the degree of similarity between samples. The three-dimensional PCA plot indicates that there was a high degree of similarity between samples within the same treatment, but much less similarity between samples from different treatments (Fig. 3A). This effect is also demonstrated by the hierarchical clustering of samples (Fig. 3B). Despite the fact that the 0- and 12-day samples clustered together on one branch and the 2- and 5-day samples clustered together on the other branch, correlation is actually low, suggesting that the samples from each time point represent unique groups (Fig. 3B).

K-means clustering was performed to group together genes with expression patterns, in response to all treatments, that were similar. We identified eight different *K*-means clusters that fell into one of three more basic expression patterns (Fig. 4). The three basic expression patterns were distinguished by their relative change in expression 2 days after surgery and are characterized by genes that increased, decreased, or showed no change.

The largest group, which consisted of clusters 1, 4, and 8 and contained 55% (507) of the genes, was characterized by an increase in expression on day 2, after which clusters 1 and 8 returned to control levels at various rates, whereas the expression of genes in cluster 4 remained high through day 12 (Fig. 5A). The second group consisted of clusters 2, 3, and 7 and contained 36% (329) of the genes (Fig. 5B). Genes in this group had an expression pattern opposite that of the first and were characterized by a decrease in expression levels on day 2. In the third group, the day-2 expression levels remained unchanged from the control levels and then increased on day 5 (Fig. 5C).

DISCUSSION

Animal Models

To make optimal use of the microarray technology for investigating a process such as bleb failure after GFS, it is necessary to generate multiple tissue samples across multiple time points.

This type of experimental design is not possible in humans—hence, the need for an animal model. It would be ideal to use a successful animal model of GFS as a control, but all existing animal models show aggressive healing, leading to eventual failure. Like other well-established animal models of GFS, our rat model exhibits relatively aggressive wound healing, which may mimic the more problematic human clinical cases.

Wound healing in the mouse after the subconjunctival injection of physiologically balanced saline[48] and scleral (needle) perforation,[49] as well as healing after the creation of a scleral wound in the rat,[50] have been described. However, we have been unable to demonstrate survival of the scleral needle tract bleb in the rat beyond 3 days.[38] Furthermore, none of the previously proposed mouse or rat models resembles current human filtering surgery as well as the new rat model used in this study, which exhibits two important features. First, it results in a filtering bleb that is sufficiently long lasting to characterize progressive bleb failure. Second, it closely mimics previous primate and rabbit models and one form of human glaucoma surgery, through the insertion of a tube into the anterior chamber and drainage of aqueous into the subconjunctival space. The model behaved in a reliable and reproducible manner, as indicated by PCA, which showed good clustering of multiple samples from various time points. Problems associated with this model are generally caused by the small size of the ocular structures and include the technical difficulty of the surgery, difficulties performing tonometry, and the small amount of tissue that is obtainable for histologic or other investigation.

Gene Expression Patterns

Microarray technology offers the unique ability to assess major trends and broad patterns of gene expression. Microarray studies are now commonly found in most areas of life science research and are an invaluable research tool. The ability to view the system at a global level by nature dictates a nonhypothetical approach. However, it is this fact and the fact that microarrays can simultaneously test all hypotheses that give this type of study its unequaled ability to look at molecular mechanisms. Gene array studies are typically designed to yield large amounts of unbiased data, identifying the differential expression of genes across biological processes and helping to
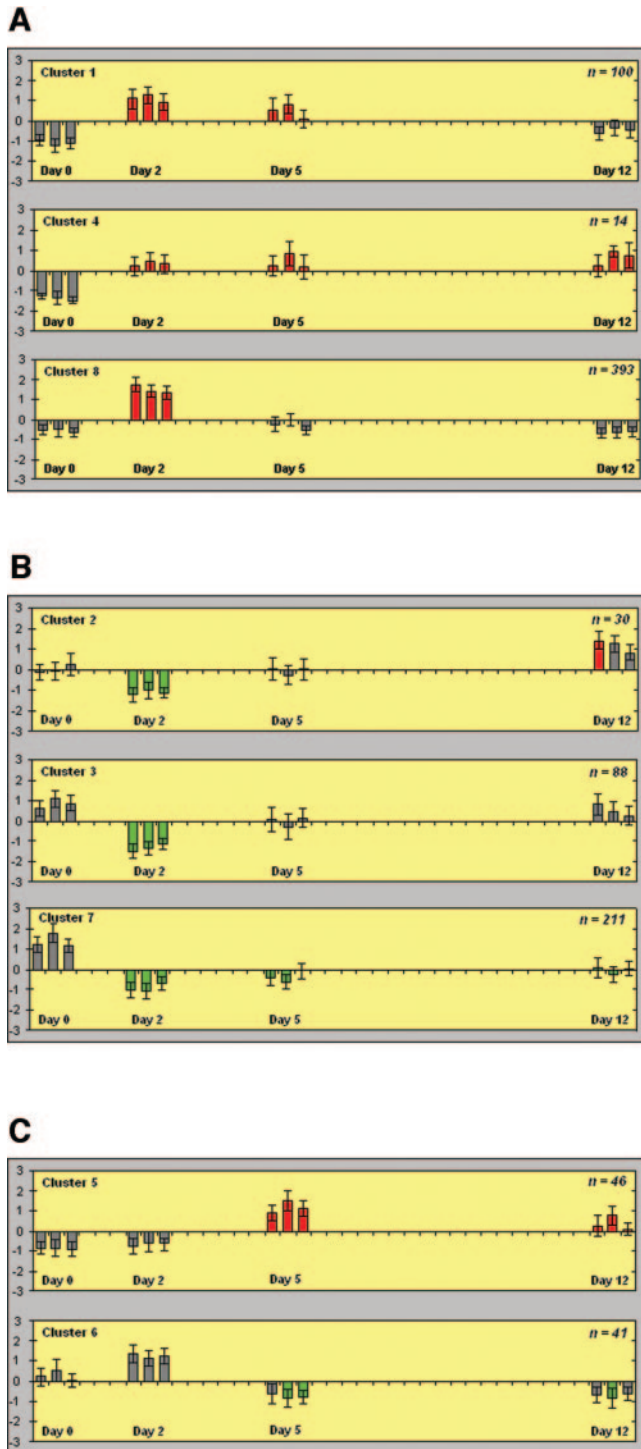
FIGURE 5. Mean expression patterns of the eight *K*-means clusters. Within a cluster, each histogram represents a sample (chip), and its height represents the mean normalized signal value of all genes in the cluster for that chip. Normalized signal value (*y*-axis) is determined on an individual gene basis and is a measure of standard deviations from the mean values across all samples. Error bars, SD. *K*-means clusters are grouped according to three basic expression patterns: (**A**) clusters that are characterized by an increase in gene expression 2 days after surgery; (**B**) clusters that are characterized by a decrease in gene expression 2 days after surgery; and (**C**) clusters that are characterized by no change in gene expression 2 days after surgery but a change on day 5. Increased expression above the control (no overlap in error bars) is represented by *red*, decreased expression by *green*, and no change relative to the control (error bar overlap) by *gray*.

generate new hypotheses. Our study was designed within this context and is an initial broad overview of a biological process. We have highlighted several groups of mediators with expression levels that are significantly altered across the course of bleb ageing in this model. It is our intention to characterize further and investigate some of the potential mediators of the bleb-scarring process identified in this study, but these experiments are beyond the scope of the current report. Further experiments to confirm the differential expression of specific genes identified in this study using the microarray technique are needed to substantiate these genes' involvement in the wound-healing process.

Despite the fact that we chose a very stringent criterion ($P < 0.005$) for significant change in gene expression, to minimize the number of false positives, 923 genes were apparently affected by GFS at this level of significance. The greatest amount of change in gene expression pattern occurred 2 days after surgery, but the expression pattern associated with each sample period was unique, based on the degree of separation between nodes in the hierarchical cluster and the grouping of samples in the principle component analysis (Fig. 3).

The genes for which there was a significant treatment effect could primarily be classified into one of three basic expression patterns: an increase on day 2; a decrease on day 2; or no change on day 2, but an increase or decrease on days 5 or 12.

On day 2, we saw an increase in the expression levels of several genes involved in the initial phases of wound healing. These included several heat-shock proteins, signaling genes such as MAPKK and FK506-binding protein 1a, cell-cycle–related proteins, and cyclins. Other genes with increased expression levels were those associated with glycolysis, as would be expected during new tissue building. The genes associated with apoptosis (predominantly the Bcl-2 and caspase families) did not show significant changes. We saw further evidence that structural changes were beginning to take place, as indicated by increases in procollagen (types 1, 2, 10, and 12), collagen (types 1, 3, 5, and 18), vimentin, integrin, fibronectin, and matrix metalloproteinase (MMP)-2, -3, -9, -13, -14, and -24. Some of the early responses, such as those of the heat-shock proteins and cell-cycle–related genes, were transient, and transcript levels returned to presurgery levels by day 5. Others, such as the procollagens (except II), the collagens, and the MMPs (except 24), remained elevated through day 12. The elevated expression of these genes at day 12 indicates that the wound-healing response continues beyond bleb failure.

Wound-Healing Patterns and Specific Genes

Tissue injury, surgical or otherwise, results in a cascade of platelet aggregation, adhesion, and degranulation and initiates a chain of cellular signaling pathways, including the local release of multiple cytokines and growth factors that activate the expression of various genes and their protein products.[51] In the rabbit model, several growth factors have already been implicated in the conjunctival scarring response after GFS. These include transforming growth factor (TGF)-β[52] and connective tissue growth factor (CTGF).[53] Based on these data, the expression of these genes was also specifically assessed.

The TGF-β family represents a group of structurally related peptide growth factors that occur in isoforms 1, 2, and 3 in mammalian tissue. As well as isoform type, translational control and activation of the latent complex are important determinants of functionality. Multiple transcripts of TGF-β2 with different abundance and sizes have been described in various tissues.[54–56] The structures of the different transcripts are largely unexplored. Both a long (2880 bp) and short (1255 bp) form of TGF-β2 have been described in rat muscle, with the long form constituting ~6% of total TGF-β2 messages.[57] TGF-β

TABLE 3. Mean Signal Values ($n = 3$) of Genes Coding for Growth Factors

Gene Name	Day 0	Day 2	Day 5	Day 12
Brain-derived neurotrophic factor	15.1	23.7	17.1	25.4
Connective tissue growth factor	75.4	205.6	391.4	205.7
Epidermal growth factor	47.2	64.1	60.1	63.2
Fibroblast growth factor 4	8.4	9.5	12.9	1.8
Fibroblast growth factor 6	16.1	40.0	23.9	27.6
Fibroblast growth factor 7	11.9	7.6	10.2	19.7
Fibroblast growth factor 10	25.5	49.8	32.6	34.6
Fibroblast growth factor 11	17.7	25.6	19.6	25.8
Fibroblast growth factor 12	22.2	34.6	26.3	29.4
Fibroblast growth factor 13	23.3	31.9	25.8	26.2
Fibroblast growth factor 14	22.6	31.5	22.0	27.5
Fibroblast growth factor 16	76.1	101.3	74.3	87.2
Fibroblast growth factor 17	22.2	26.3	31.4	27.2
Fibroblast growth factor 20	7.1	12.5	9.8	7.8
Fibroblast growth factor 22	5.6	15.3	14.9	9.9
Fibroblast growth factor 23	12.8	26.7	18.5	17.4
Hepatoma-derived growth factor	319.0	553.8	314.1	317.0
Insulin-like growth factor 1	−22.3	12.1	213.8	125.3
Insulin-like growth factor 2	8.1	17.5	11.1	4.8
Insulin-like growth factor 2	8.5	32.2	21.1	19.6
Insulin-like growth factor 2	13.3	20.1	45.7	28.8
Insulin-like growth factor 2	109.5	191.0	153.5	135.4
Lens epithelium-derived growth factor	5.8	29.1	10.7	5.7
Nerve growth factor, gamma	5.5	10.6	8.5	7.8
Placental growth factor	30.2	11.0	22.4	8.3
Placental growth factor	19.9	21.6	28.7	28.3
Platelet derived growth factor, alpha	123.6	118.5	136.1	111.9
Platelet-derived growth factor, C pp	19.6	55.7	30.8	34.0
Stem cell growth factor	4.7	5.2	32.4	23.1
Transforming growth factor alpha	57.2	63.2	38.4	39.1
Transforming growth factor beta 1	1.8	1.5	17.9	6.1
Transforming growth factor beta 2	25.3	19.6	27.2	24.3
Transforming growth factor beta 2	61.5	8.9	41.5	24.4
Transforming growth factor beta 3	11.0	39.4	78.1	63.5
Vascular endothelial growth factor	23.2	28.3	27.1	27.4
Vascular endothelial growth factor B	41.7	30.3	40.8	44.4
Vascular endothelial growth factor C	48.4	94.1	85.6	75.0

has been shown to induce cell migration,[58] scarring,[59] and wound contracture.[60] Recent work by Cordeiro et al.[61,62] has shown increased experimental bleb survival in the rabbit, with the use of injectable TGF-β2 antisense oligonucleotides, and improved bleb survival in patients, with the use of a novel, recombinant human monoclonal antibody to TGF-β2.

After GFS in our rat model, levels of TGF-β1 rose from day 0 and day 2, becoming most elevated by day 5, and decreased again by day 12 (Table 3). TGF-β2 expression was identified by two different probe sets (Affymetrix IDs 1387172 and 1388011) that may represent splice variants of the same gene. We interpret the first ID annotation to be representative of the long form of TGF-β2. This indicated an initially high level, falling by day 2 and returning to baseline on days 5 and 12. The second annotation, we interpret to represent either the short form of TGF-β2 or a combination of the two forms and as such, to be more representative of overall TGF-β2 expression. This peaked by day 5, returning to baseline by day 12. This finding mirrors our previous ELISA data from the rabbit model, which showed peak TGF-β2 levels on day 5.[38]

TGF-β3 expression increased from day 0, reaching a peak by day 5, and remained elevated above baseline on day 12. TGF-β3 has been associated with scarless healing in skin.[63]

CTGF has been found to act as a mitogen in fibroblast cell cultures and to upregulate components of the extracellular matrix (ECM), such as collagen, integrin, and fibronectin.[64] CTGF has also been shown to be a downstream mediator of TGF-β.[65–69] In keeping with our understanding of the role these growth factors play in bleb failure, we found that the

CTGF increased from baseline to reach maximum expression by day 5 after surgery, with a more than fivefold increase in levels. It decreased again by day 12 but remained above baseline levels. This pattern is again in close accord with our previous work examining CTGF levels by ELISA after GFS in the rabbit model. Other growth factors with expression changes after GFS included multiple members of both the fibroblast growth factor (FGF) and insulin-like growth factor (IGF) families (Table 3).

After the acute inflammatory phase, re-epithelialization, angiogenesis, and granulation occur. New vasculature facilitates the migration of fibroblasts into the wound bed, in response to cytokines and growth factors, where they proliferate and synthesize collagen and other components of the new ECM, including proteoglycans.[70,71]

Collagens are the structural proteins that provide tensile strength to the wound. Collagen synthesis as well as fibril diameter has been shown to increase in response to mechanical stress.[72,73] The basic structure of proteoglycans includes a core protein and at least one (but usually more) carbohydrate chains, the so-called glycosaminoglycans (GAGs). These provide hydration to the cornea and conjunctiva,[74,75] and GAG alterations associated with healing in the cornea have been reported.[76] It is the maturation and organization of the synthesized collagen that results in the formation of scar tissue, and the changes observed in the expression of products such as lumican, biglycan, vimentin, and fibronectin are consistent with changes that would be expected as the conjunctival wound forms a scar and contracts. Integrins and fibronectin

TABLE 4. Mean Signal Values ($n = 3$) of Genes Coding for Structural Proteins

Gene Name	Day 0	Day 2	Day 5	Day 12
Aggrecan 1	24.7	22.1	32.6	15.3
Basigin	649.0	731.8	742.6	660.8
Brevican	18.2	27.6	20.9	21.7
Cathepsin E	23.5	20.9	27.2	43.8
Cerebroglycan	24.6	22.7	22.2	22.9
Collagen, type I, alpha 1	79.8	208.7	1251.5	1032.3
Collagen, type I, alpha 1	41.4	133.0	841.0	688.1
Collagen, type III, alpha 1	143.7	478.9	1486.7	1406.3
Collagen, type V, alpha 1	37.7	58.4	313.1	228.6
Collagen, type V, alpha 1	19.7	36.6	180.7	122.7
Collagen, type V, alpha 2	45.8	136.7	522.9	414.1
Collagen, type V, alpha 2	29.2	69.1	342.5	312.7
Collagen, type V, alpha 3	2.4	13.5	163.3	127.9
Collagen, type XVIII, alpha 1	20.6	281.7	187.2	83.9
Collagen, type XVIII, alpha 1	−18.1	112.6	74.8	6.5
Decorin	342.3	417.0	878.9	716.3
Fibromodulin	18.6	28.2	73.5	54.5
Fibronectin 1	45.9	232.3	789.5	718.4
F-spondin	24.1	34.6	55.1	71.3
Glypican 1	125.1	179.7	244.3	180.6
Glypican 3	125.6	124.3	116.4	143.0
Integrin alpha 1	18.4	43.8	34.7	36.9
Laminin, beta 2	48.7	32.8	51.4	47.3
Netrin 1	10.0	17.4	30.9	25.8
Procollagen, type I, alpha 2	55.9	168.6	1051.7	803.3
Procollagen, type I, alpha 2	98.5	206.6	1244.5	973.6
Procollagen, type I, alpha 2	134.4	195.1	125.8	116.9
Procollagen, type II, alpha 1	32.8	53.0	43.6	36.8
Procollagen, type II, alpha 1	8.4	8.5	14.6	8.0
Procollagen, type X, alpha 1	6.2	8.6	18.4	10.3
Procollagen, type XI, alpha 1	0.1	−0.1	12.2	6.4
Procollagen, type XII, alpha 1	12.2	15.6	52.9	30.0
Syndecan 4	744.9	693.4	661.3	691.7
Vimentin	166.5	602.9	926.6	627.8
Vitronectin	6.2	10.0	11.2	13.8

play crucial roles in cell adhesion, migration, and signaling by providing transmembrane links between the extracellular matrix and the cytoskeleton and generating cell–matrix adhesions.[77,78]

Vimentin is a widely expressed intermediate filament protein, involved mainly in structural processes and wound healing and plays an important role in mechanical and biological functions, such as cell contractility, migration, stiffness, stiffening, and proliferation.[79] Vimentin is secreted by macrophages in response to proinflammatory signaling pathways. Extracellular vimentin also has a bacteriocidal function,[80] and it has been used as a marker for myofibroblasts (MFBs).[81]

Changes in expression of multiple structural proteins and components of the ECM were noted in our model (Table 4). Fivefold or greater increases were seen in procollagen 1; collagens 1, 3, and 18; vimentin; and fibronectin (Table 2).

Substantial evidence indicates that wound contraction in connective tissues is cell mediated and that the active cell type is a modified contractile fibroblast, the MFB.[82–85] MFBs contain the contractile apparatus of smooth muscle cells, α-smooth muscle actin (αSMA), and can be identified by its presence.[86,87] As repair progresses, fibroblasts display increased expression levels of adhesion molecules and assume an MFB phenotype, mediated in part by TGF-β, to facilitate wound contraction.[88] Contractile fibroblasts have been identified in contracting wounds in the cornea and conjunctiva.[89,90] In our array results, αSMA activity was noted to increase from day 0 to a peak at day 5 essentially doubling in expression and beginning to fall again by day 12.

The final phase of wound maturation is the degradation and reorganization of fibrillar collagen and other matrix proteins.

This function is assisted by a family of structurally related proteolytic enzymes, the MMPs. More than 20 different MMPs have been identified. Structural differences between MMPs confer substrate specificity, regulate binding to matrix proteins, and determine interactions with the tissue inhibitors of metalloproteinases (TIMPs), which inhibit MMP activity.[91]

MMPs may degrade multiple substrates, with substrate overlap between individual MMPs. Most MMPs are not expressed in normal tissues but are transcribed in response to stimuli such as inflammatory cytokines and growth factors. Multiple cell types, including macrophages, fibroblasts, neutrophils, epithelial cells, and endothelial cells can synthesize MMPs. MMP inhibition has been shown to modulate postoperative scarring after experimental glaucoma filtration surgery.[92] In our model, we noted a more than fivefold increase in the expression of MMP-2, -3, and -9 (gelatinase B). After GFS, gelatinase B exhibits the ability to degrade components of the ECM and regulates the activity of a number of soluble proteins.[93–96] The expression of MMP-9 was indicated by Affymetrix IDs 1369166 and 1398275, which we interpret to represent two transcript variants of the gene. Both of these rose from baseline levels to peak at day 5 and subside again at 12. The gene expression of MMP-2, -3, and -9 as well as those of the other MMPs identified and the TIMPs is presented in Table 5.

As well as factors that may have been anticipated to fit our proposed model, we noted significant changes in expression (fivefold or greater) in multiple genes whose role in the healing conjunctival environment has not been previously examined. These included breast cancer susceptibility gene 1 (BRCA1)–associated RING domain, cysteine-rich protein 2 (CRP2), renin I, polo-like kinase, members of the serine/threonine kinase

TABLE 5. Mean Signal Values ($n = 3$) of Genes Coding for Matrix Metalloproteinases

Gene Name	Day 0	Day 2	Day 5	Day 12
Matrix metalloproteinase 2 (type IV collagenase)	44.7	93.5	332.7	329.4
Matrix metalloproteinase 3	56.3	217.0	291.9	140.1
Matrix metalloproteinase 9 (gelatinase B, type IV collagenase)	0.7	23.7	26.8	4.9
Matrix metalloproteinase 9 (gelatinase B, type IV collagenase)	4.5	42.3	52.1	11.7
Matrix metalloproteinase 11 (stromelysin 3)	−1.5	−5.9	11.0	12.8
Matrix metalloproteinase 12	−10.0	−40.2	21.2	46.9
Matrix metalloproteinase 13	3.9	77.9	66.9	33.2
Matrix metalloproteinase 14, membrane-inserted	109.4	216.5	464.6	404.8
Matrix metalloproteinase 23	−1.6	−9.0	24.8	18.5
Matrix metalloproteinase 24 (membrane-inserted)	15.2	20.4	17.9	17.0
Matrix metalloproteinase 24 (membrane-inserted)	119.6	109.8	144.7	129.9
Matrix metalloproteinase 24 (membrane-inserted)	56.9	53.3	67.2	78.0
Tissue inhibitor of metalloproteinase 1	58.9	331.5	437.5	190.4
Tissue inhibitor of metalloproteinase 2	49.8	35.3	82.5	104.3
Tissue inhibitor of metalloproteinase 2	338.3	266.5	507.6	482.2
Tissue inhibitor of metalloproteinase 2	621.1	556.7	784.1	701.6
Tissue inhibitor of metalloproteinase 2	255.3	184.0	333.4	334.2
Tissue inhibitor of metalloproteinase 3	5.5	9.1	14.6	13.2
Tissue inhibitor of metalloproteinase 3	30.4	29.3	51.3	60.8
Tissue inhibitor of metalloproteinase 3	70.7	116.0	132.4	120.3

family, Kruppel-like factors (KLFs), and the asialoglycoprotein receptor (ASGPR).

Breast cancer susceptibility gene 1 (BRCA1)–associated RING domain (BARD1) was discovered as a protein interacting with the RING domain of BRCA1. Colocalization of BARD1 with BRCA1 and other repair proteins has been shown to indicate a DNA repair function.[97] In vertebrates, members of the CRP family mediate protein–protein interactions and are of fundamental importance for cell proliferation, cell differentiation, cytoskeletal remodeling, and transcriptional regulation.[98] CRP proteins contain domains necessary for protein–protein interactions.[99] The polo-like kinase family is involved in many aspects of the cell cycle, such as activation of Cdc2, centrosome assembly and maturation, activation of the anaphase-promoting complex (APC) during the metaphase-anaphase transition, and cytokinesis.[100] The serine/threonine kinase Akt, or protein kinase B (PKB), lies at the crossroads of multiple cellular signaling pathways and acts as a transducer of many functions initiated by growth factor receptors.[101] KLFs are highly related proteins that are important components of cellular transcriptional machinery. By regulating the expression of a large number of genes, KLF transcription regulators may take part in virtually all facets of cellular function, including cell proliferation, apoptosis, differentiation, and neoplastic transformation.[102] The ASGPR is a prototype of the class of receptors that enters cells and delivers ligand to intracellular compartments.[103] This receptor has been identified as a good indicator of periportal and/or bridging necrosis and fibrosis in hepatic research.[104,105] It is also involved in the in vitro clearance of apoptotic bodies.[106]

CONCLUSIONS

To our knowledge, this study represents the first time a broad spectrum of gene expression after GFS in an animal model has been examined. This microarray analysis represents an initial step in a series of experiments to determine the roles and mechanisms of various mediators of the bleb-scarring process. Other steps may involve protein assays and interventional studies. The identification of key mediators of the wound-healing process may lead to the development of further novel and specific treatments that could improve long-term surgical outcomes and perhaps avoid the unwanted side effects of the currently used, relatively nonspecific antimetabolites.

References

1. Roodhooft JM. Leading causes of blindness worldwide. *Bull Soc Belge Ophtalmol* 2002;283:19–25.
2. Quigley HA. Number of people with glaucoma worldwide. *Br J Ophthalmol.* 1996;80:389–393.
3. Pizzarello L, Abiose A, Ffytche T, et al. VISION—The Right to Sight: a global initiative to eliminate avoidable blindness. *Arch Ophthalmol.* 2004;122:615–620.
4. Lichter PR, Musch DC, Gillespie BW, et al. for theCIGTS Study Group. Interim clinical outcomes in the Collaborative Initial Glaucoma Treatment Study comparing initial treatment randomized to medications or surgery. *Ophthalmology.* 2001;108:1943-1953.
5. Leskea MC, Heijl A, Hyman L, Bengtsson B, Komaroff E. Factors for progression and glaucoma treatment: The Early Manifest Glaucoma Trial. *Curr Opin Ophthalmol.* 2004;15:102–106.
6. The American Academy of Ophthalmology. *Preferred Practice Patterns: Primary Angle Closure, Primary Open-Angle Glaucoma and Primary Open-Angle Glaucoma Suspect).* San Francisco: American Academy of Ophthalmology. 2003.
7. Addicks EM, Quigley A, Green WR, Robin AL. Histologic characteristics of filtering blebs in glaucomatous eyes. *Arch Ophthalmol.* 1983;101:795-798.
8. Hitchings RA, Grierson I. Clinico pathological correlation in eyes with failed fistulizing surgery. *Trans Ophthalmol Soc UK.* 1983; 103:84–88.
9. Lama PJ, Fechtner RD. Antifibrotics and wound healing in glaucoma surgery. *Surv Ophthalmol.* 2003;48:314–346.
10. Skuta GL. Antifibrotic agents in glaucoma filtering surgery (review). *Int Ophthalmol Clin.* 1993;33:165–182.
11. Rockwood EJ, Parrish RK II, Heuer DK, et al. Glaucoma filtering surgery with 5-fluorouracil. *Ophthalmology.* 1987;94:1071-1078.
12. Stamper RL, McMenemy MG, Lieberman MF. Hypotonous maculopathy after trabeculectomy with subconjunctival 5-fluorouracil. *Am J Ophthalmol.* 1992;114,544–553.
13. Jampel HD, Pasquale LR, Dibernardo C. Hypotony maculopathy following trabeculectomy with mitomycin C (letter). *Arch Ophthalmol.* 1992;110:1049–1050.

14. Greenfield DS, Liebmann JM, Jee J, Ritch R. Late-onset bleb leaks after glaucoma filtering surgery. *Arch Ophthalmol.* 1998;116:443–447.

15. Mietz H, Addicks K, Bloch W, Krieglstein G. Long-term intraocular toxic effects of topical mitomycin C in rabbits. *J Glaucoma.* 1996;5:325–333.

16. Wolner B, Liebmann JM, Sassani JW, et al. Late bleb-related endophthalmitis after trabeculectomy with adjunctive 5-fluorouracil. *Ophthalmology.* 1991;98:1053–1060.

17. Waheed S, Liebmann JM, Greenfield DS, et al. Recurrent bleb infections. *Br J Ophthalmol.* 1998;82:926–929.

18. Soltau JB, Rothman RF, Budenz DL, et al. Risk factors for glaucoma filtering bleb infections. *Arch Ophthalmol.* 2000;118:338–342.

19. Tsou R, Cole JK, Nathens AB, et al. Analysis of hypertrophic and normal scar gene expression with cDNA microarrays. *J Burn Care Rehabil.* 2000;21:541–550.

20. Lo WR, Rowlette LL, Caballero M, Yang P, Hernandez MR, Borras T. Tissue differential microarray analysis of dexamethasone induction reveals potential mechanisms of steroid glaucoma. *Invest Ophthalmol Vis Sci.* 2003;44:473–485.

21. Hernandez MR, Agapova OA, Yang P, Salvador-Silva M, Ricard CS, Aoi S. Differential gene expression in astrocytes from human normal and glaucomatous optic nerve head analyzed by cDNA microarray. *Glia.* 2002;38:45–64.

22. Wiechmann AF. Regulation of gene expression by melatonin: a microarray survey of the rat retina. *J Pineal Res.* 2002;33:178–185.

23. Richey KJ, Engrav LH, Pavlin EG, Murray MJ, Gottlieb JR, Walkinshaw MD. Topical growth factors and wound contraction in the rat: Part I. Literature review and definition of the rat model. *Ann Plast Surg.* 1989;23:159–165.

24. Engrav LH, Richey KJ, Kao CC, Murray MJ. Topical growth factors and wound contraction in the rat: Part II. Platelet-derived growth factor and wound contraction in normal and steroid-impaired rats. *Ann Plast Surg.* 1989;23:245–248.

25. Young W. Spinal cord contusion models (review). *Prog Brain Res.* 2002;137:231–255

26. Meddahi A, Caruelle JP, Gold L, Rosso Y, Barritault D. New concepts in tissue repair: skin as an example (review). *Diabetes Metab.* 1996;22:274–278.

27. Ashhurst DE. Collagens synthesized by healing fractures (review). *Clin Orthop.* 1990;255:273–283.

28. Varela JC, Goldstein MH, Baker HV, Schultz GS. Microarray analysis of gene expression patterns during healing of rat corneas after excimer laser photorefractive keratectomy. *Invest Ophthalmol Vis Sci.* 2002;43:1772–1782.

29. Fini ME, Girard MT, Matsubara M. Collagenolytic/gelatinolytic enzymes in corneal wound healing (review). *Acta Ophthalmol Suppl.* 1992;202:26–33.

30. Yamada J, Dana MR, Sotozono C, Kinoshita S. Local suppression of IL-1 by receptor antagonist in the rat model of corneal alkali injury. *Exp Eye Res.* 2003;76:161–167.

31. WoldeMussie E, Yoles E, Schwartz M, Ruiz G, Wheeler LA. Neuroprotective effect of memantine in different retinal injury models in rats. *J Glaucoma.* 2002;11:474–480.

32. Cordeiro MF, Constable PH, Alexander RA, Bhattacharya SS, Khaw PT. Effect of varying the mitomycin-C treatment area in glaucoma filtration surgery in the rabbit. *Invest Ophthalmol Vis Sci.* 1997;38:1639–1646.

33. Gwin TD, Stewart WC, Gwynn DR. Filtration surgery in rabbits treated with diclofenac or prednisolone acetate. *Ophthalmic Surg.* 1994;25:245–250.

34. Doyle JW, Sherwood MB, Khaw PT, McGrory S, Smith MF. Intraoperative 5-fluorouracil for filtration surgery in the rabbit. *Invest Ophthalmol Vis Sci.* 1993;34:3313–3139.

35. Connon CJ, Meek KM. Organization of corneal collagen fibrils during the healing of trephined wounds in rabbits. *Wound Repair Regen.* 2003;11:71–78.

36. Gao J, Gelber-Schwalb TA, Addeo JV, Stern ME. Apoptosis in the rabbit cornea after photorefractive keratectomy. *Cornea.* 1997;16:200–208.

37. Schultz G, Khaw PT, Oxford K, MaCauley S, Van Setten G, Chegini N. Growth factors and ocular wound healing (review). *Eye.* 1994;8:184–187.

38. Lloyd MA, Baerveldt G, Nguyen QH, Minckler DS. Long-term histologic studies of the Baerveldt implant in a rabbit model. *J Glaucoma.* 1996;5:334–339.

39. Miller MH, Grierson I, Unger WI, Hitchings RA. Wound healing in an animal model of glaucoma fistulizing surgery in the rabbit. *Ophthalmic Surg.* 1989;20:350–357.

40. Wilson AS, Hobbs BG, Speed TP, Rakoczy PE. The microarray: potential applications for ophthalmic research. *Mol Vis.* 2002;8:259–270.

41. Wang P, Ding F, Chiang H, Thompson RC, Watson SJ, Meng F. ProbeMatchDB: a Web database for finding equivalent probes across microarray platforms and species. *Bioinformatics.* 2002;18:488–489.

42. Birney E, Clamp M, Hubbard T. Databases and tools for browsing genomes. *Annu Rev Genomics Hum Genet.* 2002;3:293–310.

43. Hanna KD, Pouliquen YM, Savoldelli M, et al. Corneal wound healing in monkeys 18 months after excimer laser photorefractive keratectomy. *Refract Corneal Surg.* 1990;6:340–345.

44. Gressel MG, Parrish RK II, Folberg R. 5-Fluorouracil and glaucoma filtering surgery: I. An animal model. *Ophthalmology.* 1984;91:378–383.

45. Bair JS, Chen CW. Trabeculectomy with multiple applications of mitomycin-C in monkeys with experimental glaucoma. *J Ocul Pharmacol Ther.* 1997;13:115–128.

46. Hasty B, Heuer DK, Minckler DS. Primate trabeculectomies with 5-fluorouracil collagen implants. *Am J Ophthalmol.* 1990;109:721–725.

47. Esson D, Neelakantan A, Sherwood M. A new model of glaucoma filtering surgery in the rat. *J Glaucoma.* 2004;13:407–412.

48. Reichel MB, Cordeiro MF, Alexander RA, et al. New model of conjunctival scarring in the mouse eye. *Br J Ophthalmol.* 1998;82:1072–1077.

49. Mietz H, Chevez-Barrios P, Lieberman MW. A mouse model to study the wound healing response following filtration surgery. *Graefes Arch Clin Exp Ophthalmol.* 1998;236:467–475.

50. Sheridan CM, Unger WG, Ayliffe W, et al. Macrophages during fibrosis following scleral fistulising surgery in a rat model. *Curr Eye Res.* 1996;15:559–568.

51. Singer AJ, Clark RA. Cutaneous wound healing. *N Engl J Med.* 1999;341:738–746.

52. Khaw PT, Occleston NL, Schultz G, Grierson I, Sherwood MB, Larkin G. Activation and suppression of fibroblast function. *Eye.* 1994;8:188–195.

53. Esson D, Schultz G, Sherwood M, et al. Expression of connective tissue growth factor (CTGF) after glaucoma filtration surgery in a rabbit model. *Invest Ophthalmol Vis Sci.* 2004;45:485–491.

54. Schmid P, Cox X, Bilbe G, Maier R, McMaster G.K. Differential expression of TGF beta 1, beta 2, and beta 3 genes during mouse embryogenesis. *Development.* 1991;111:117–130.

55. McLennan IS, Koishi K, Zhang M, Murakami N. The non-synaptic expression of transforming growth factor–beta2 is neurally regulated and varies between skeletal muscle fibre types. *Neuroscience.* 1998;87:845–853.

56. Miller DA, Lee A, Pelton RW, Chen EY, Moses HL, Derynck R. Murine transforming growth factor–beta2 cDNA sequence and expression in adult tissues and embryos. *Mol Endocrinol.* 1989;3:1108–1114.

57. Koishi K, Dalzell KG, McLennan IS. The expression and structure of TGF-beta2 transcripts in rat muscles. *Biochim Biophys Acta.* 2000;1492:311–319.

58. Parekh T, Saxena B, Reibman J, Cronstein BN, Gold LI. Neutrophil chemotaxis in response to TGF-beta isoforms (TGF-beta 1, TGF-beta 2, TGF-beta 3) is mediated by fibronectin. *J Immunol.* 1994;152:2456–2466.

59. Cordeiro M, Bhattacharya S, Schultz G, et al. TGF-β1, -β2 and -β3 in vitro: biphasic effects on Tenon's fibroblast contraction, proliferation and migration. *Invest Ophthalmol Vis Sci.* 2000;41:756–763.

60. Pena RA, Jerdan JA, Glaser BM. Effects of TGF-beta and TGF-beta neutralizing antibodies on fibroblast-induced collagen gel

contraction: implications for proliferative vitreoretinopathy. *Invest Ophthalmol Vis Sci.* 1994;35:2804–2808.

61. Cordeiro MF, Mead A, Ali RR, et al. Novel antisense oligonucleotides targeting TGF-beta inhibit in vivo scarring and improve surgical outcome. *Gene Ther.* 2003;10:59–71.

62. Cordeiro MF, Gay JA, Khaw PT. Human anti-transforming growth factor-beta2 antibody: a new glaucoma anti-scarring agent. *Invest Ophthalmol Vis Sci.*1999;40:2225–2234.

63. Niesler CU, Ferguson MWJ. TGF-beta superfamily cytokines in wound healing. In: Brei, SN, Wahl SM, eds. *TGF-beta and Related Cytokines in Inflammation.* Basel, Switzerland: Birkhauser, 2001;173–198.

64. Frazier K, Williams S, Kothapalli D, Klapper H, Grotendorst GR. Stimulation of fibroblast cell growth, matrix production, and granulation tissue formation by connective tissue growth factor. *J Invest Dermatol.* 1996;107:404–411.

65. Duncan MR, Frazier KS, Abramson S, et al. Connective tissue growth factor mediates transforming growth factor beta-induced collagen synthesis: down-regulation by cAMP. *FASEB J.* 1999;13:1774–1786.

66. Grotendorst GR. Connective tissue growth factor: a mediator of TGF-beta action on fibroblasts (review). *Cytokine Growth Factor Rev.* 1997;8:171–179.

67. Ihn H. Pathogenesis of fibrosis: role of TGF-beta and CTGF. *Curr Opin Rheumatol.* 2002;14:681–685.

68. Kucich U, Rosenbloom JC, Herrick DJ, et al. Signaling events required for transforming growth factor-beta stimulation of connective tissue growth factor expression by cultured human lung fibroblasts. *Arch Biochem Biophys.* 2001;395:103–112.

69. Leask A, Holmes A, Black CM, Abraham DJ. Connective tissue growth factor gene regulation: requirements for its induction by transforming growth factor-beta 2 in fibroblasts. *J Biol Chem.* 2003;278:13008–13015.

70. McCartney-Francis NL, Frazier-Jessen M, Wahl SM. TGF-beta: a balancing act. *Int Rev Immunol.* 1998;16:553–580.

71. Birk DE, Trelstad RL. Fibroblasts compartmentalize the extracellular space to regulate and facilitate collagen fibril, bundle, and macroaggregate formation. In: Raddi EH, ed. *Extracellular Matrix: Structure and Function.* New York: Alan R. Liss; 1985: 373–382.

72. Sanders JE, Goldstein BS. Collagen fibril diameters increase and fibril densities decrease in skin subjected to repetitive compressive and shear stresses. *J Biomech.* 2001;34:1581–1587.

73. Breen EC. Mechanical strain increases type I collagen expression in pulmonary fibroblasts in vitro. *J Appl Physiol.* 2000;88:203–209.

74. Saika S, Ohnishi Y, Ooshima A, Liu CY, Kao WW. Epithelial repair: roles of extracellular matrix. *Cornea.* 2002;21:S23–S29.

75. Meek KM, Leonard DW, Connon CJ, Dennis S, Khan S. Transparency, swelling and scarring in the corneal stroma. *Eye.* 2003;17:927–936.

76. Hsu WC, Spilker MH, Yannas IV, Rubin PA. Inhibition of conjunctival scarring and contraction by a porous collagen-glycosaminoglycan implant. *Invest Ophthalmol Vis Sci.* 2000;41:2404–2411.

77. Robinson EE, Foty RA, Corbett SA. Fibronectin matrix assembly regulates α5β1-mediated cell cohesion. *Mol Biol Cell.* 2004;15:973–981.

78. Yamada KM, Pankov R, Cukierman E. Dimensions and dynamics in integrin function. *Braz J Med Biol Res.* 2003;36:959–966.

79. Wang J, Chen H, Seth A, McCulloch CA. Mechanical force regulation of myofibroblast differentiation in cardiac fibroblasts. *Am J Physiol.* 2003;285:H1871–H1881

80. Mor-Vaknin N, Punturieri A, Sitwala K, Markovitz DM. Extracellular vimentin also has a bacteriocidal function. *Nat Cell Biol.* 2003;5:59–63.

81. Whiting CV, Tarlton JF, Bailey M, Morgan CL, Bland PW. Abnormal mucosal extracellular matrix deposition is associated with increased TGF-beta receptor-expressing mesenchymal cells in a mouse model of colitis. *J Histochem Cytochem.* 2003;51:1177–1189.

82. Abercrombie M, James DW, Newcombe JF. Wound contraction in rabbit skin, studied by splinting the wound margins. *J Anat.* 1960;94:170–182.

83. Higton DIR, James DW. The force of contraction of full-thickness wounds of rabbit skin. *Br J Surg.* 1964;51:462–466.

84. Majno G, Gabbiani G, Hirchel BJ, Ryan GB, Statkov PR. Contraction of granulation tissue in vitro: similarity to smooth muscle. *Science.* 1971;173:548–550.

85. Gabbiani G, Ryan GB, Majno G. Presence of modified fibroblasts in granulation tissue and their possible role in wound contraction *Experientia.* 1971;27:549–550.

86. Masur SK, Dewal HS, Dinh TT, Erenburg I, Petridou S. Myofibroblasts differentiate from fibroblasts when plated at low density. *Proc Natl Acad Sci USA.*1996;93:4219–4223.

87. Jester JV, Petroll WM, Barry PA, Cavanagh HD. Expression of alpha-smooth muscle (alpha-SM) actin during corneal stromal wound healing. *Invest Ophthalmol Vis Sci.* 1995;36:809–819.

88. Grotendorst GR, Rahmanie H, Duncan MR. Combinatorial signaling pathways determine fibroblast proliferation and myofibroblast differentiation. *FASEB J.* 2004;18:469–479.

89. Peiffer RL, Lipper S, Merrit JC. Myofibroblasts in the healing of filtering wounds in rabbit, dog, and cat. *Glaucoma.* 1981;3:277–280.

90. Miller MH, Grierson I, Unger WI, Hitchings RA. Wound healing in an animal model of glaucoma fistulizing surgery in the rabbit. *Ophthalmic Surg.*1989;20:350–357.

91. Daniels JT, Cambrey AD, Occleston NL, et al. Matrix metalloproteinase inhibition modulates fibroblast-mediated matrix contraction and collagen production in vitro. *Invest Ophthalmol Vis Sci.* 2003;44:1104–1110.

92. Wong TT, Mead AL, Khaw PT. Matrix metalloproteinase inhibition modulates postoperative scarring after experimental glaucoma filtration surgery. *Invest Ophthalmol Vis Sci.* 2003;44:1097–1103.

93. St-Pierre Y, Van Themsche C, Esteve PO. Emerging features in the regulation of MMP-9 gene expression for the development of novel molecular targets and therapeutic strategies. *Curr Drug Targets Inflamm Allergy.* 2003;2:206–215.

94. Van den Steen PE, Dubois B, Nelissen I, Rudd PM, Dwek RA, Opdenakker G. Biochemistry and molecular biology of gelatinase B or matrix metalloproteinase-9 (MMP-9). *Crit Rev Biochem Mol Biol.* 2002;37:375–536.

95. Atkinson JJ, Senior RM. Matrix metalloproteinase-9 in lung remodeling. as well as pulmonary fibrosis. *Am J Respir Cell Mol Biol.* 2003;28:12–24.

96. Pflugfelder SC, Solomon A, Dursun D, Li DQ. Dry eye and delayed tear clearance: "a call to arms." *Adv Exp Med Biol.* 2002;506:739–743.

97. Irminger-Finger I, Leung WC, Li J, et al. Identification of BARD1 as mediator between proapoptotic stress and p53-dependent apoptosis. *Mol Cell.* 2001;8:1255–1266.

98. Weiskirchen R, Gunther K. The CRP/MLP/TLP family of LIM domain proteins: acting by connecting. *Bioessays.* 2003;25:152–162.

99. Bonnin MA, Edom-Vovard F, Kefalas P, Duprez D. CRP2 transcript expression pattern in embryonic chick limb. *Mech Dev.* 2002;116:151–155.

100. Liu X, Erikson RL. Polo-like kinase 1 in the life and death of cancer cells. *Cell Cycle.* 2003;2:424–425

101. Kandel ES, Hay N. The regulation and activities of the multifunctional serine/threonine kinase Akt/PKB. *Exp Cell Res.* 1999;253:210–229.

102. Kaczynski J, Cook T, Urrutia R. Sp1- and Kruppel-like transcription factors. *Genome Biol.* 2003;4:206.

103. Stockert RJ. The asialoglycoprotein receptor: relationships between structure, function, and expression. *Physiol Rev.* 1995;75:591–609.

104. Sugahara K, Togashi H, Takahashi K, et al. Separate analysis of asialoglycoprotein receptors in the right and left hepatic lobes using Tc-GSA SPECT. *Hepatology.* 2003;38:1401–1409.

105. Eisenberg C, Seta N, Appel M, Feldmann G, Durand G, Feger J. Asialoglycoprotein receptor in human isolated hepatocytes from normal liver and its apparent increase in liver with histological alterations. *J Hepatol.* 1991;13:305–309.

106. Casey CA, McVicker BL, Donohue TM Jr, McFarland MA, Wiegert RL, Nanji AA. Liver asialoglycoprotein receptor levels correlate with severity of alcoholic liver damage in rats. *J Appl Physiol.* 2004 Jan;96:76–80.